

Journal of Biomaterials Science: Polymer Edition

Into The Groove: Instructive Conductive Silk Films With Topological Guidance Cues Direct DRG Neurite Outgrowth --Manuscript Draft--

Manuscript Number:	
Full Title:	Into The Groove: Instructive Conductive Silk Films With Topological Guidance Cues Direct DRG Neurite Outgrowth
Short Title:	Groovy Conducting Silk Films Direct Neurites
Article Type:	Short Communication
Keywords:	silk; biomaterials; neural; tissue engineering; topography
Corresponding Author:	John George Hardy, Ph.D. University of Florida Gainesville, Florida UNITED STATES
Corresponding Author Secondary Information:	
Corresponding Author's Institution:	University of Florida
Corresponding Author's Secondary Institution:	
First Author:	John George Hardy, Ph.D.
First Author Secondary Information:	
Order of Authors:	John George Hardy, Ph.D. Zin Z Khaing, Ph.D. Shangjing Xin, B.S. Lee W Tien, PhD Chiara E Ghezzi, PhD David J Mouser, B.S. Rushi C Sukhvasi, B.S. Rucsanda C Preda, B.S. Eun S Gil, PhD David L Kaplan, PhD Christine E Schmidt, PhD
Order of Authors Secondary Information:	
Manuscript Region of Origin:	UNITED STATES
Abstract:	Instructive biomaterials capable of controlling the behaviour of the cells are particularly interesting scaffolds for tissue engineering and regenerative medicine. Novel biomaterials are particularly important in societies with rapidly aging populations, where demand for organ/tissue donations is greater than their supply. Herein we describe the preparation of electrically conductive silk film-based nerve tissue scaffolds that are manufactured using all aqueous processing. Aqueous solutions of Bombyx mori silk were cast on flexible polydimethylsiloxane substrates with micrometer-scale grooves on their surfaces, allowed to dry, and annealed to impart β -sheets to the silk which assures that the materials are stable for further processing in water. The silk films were rendered conductive by generating an interpenetrating network of polypyrrole and polystyrenesulfonate in the silk matrix. Films were incubated in an aqueous solution of pyrrole (monomer), polystyrenesulfonate (dopant) and iron chloride (initiator), after which they were thoroughly washed to remove low molecular

weight components (monomers, initiators, and oligomers) and dried, yielding conductive films with sheet resistances of $124 \pm 23 \text{ k}\Omega \text{ square}^{-1}$. The micrometer-scale grooves that are present on the surface of the films are analogous to the natural topography in the extracellular matrix of various tissues (bone, muscle, nerve, skin) to which cells respond. Dorsal Root Gangions (DRGs) adhere to the films and the grooves in the surface of the films instruct the aligned growth of processes extending from the DRGs. Such materials potentially enable the electrical stimulation of cells cultured on them, and future in vitro studies will focus on understanding the interplay between electrical and topographical cues on the behaviour of cells cultured on them.

Into The Groove: Instructive Conductive Silk Films With Topological Guidance Cues Direct DRG Neurite Outgrowth

John G. Hardy,^{a,b,c,*} Zin Z. Khaing,^{a,b,*} Shangjing Xin,^a Lee W. Tien,^c
Chiara E. Ghezzi,^c David J. Mouser,^b Rushi C. Sukhavasi,^b Rucsanda C.
Preda,^c Eun S. Gil,^c David L. Kaplan,^{c,*} Christine E. Schmidt.^{a,b,*}

a) J. Crayton Pruitt Family Department of Biomedical Engineering, University of Florida, Gainesville, FL 32611, USA.

b) Department of Biomedical Engineering, The University of Texas at Austin, Austin, TX 78712, USA.

c) Department of Biomedical Engineering, Tufts University, Medford, MA 02155, USA.

* To whom correspondence should be addressed: Tel: 001-352-273-9222; Fax: 001-352-273-9221; e-mail: johnhardyuk@gmail.com (or) zink@uw.edu (or) david.kaplan@tufts.edu (or) schmidt@ufl.edu

Into The Groove: Instructive Conductive Silk Films With Topological Guidance Cues Direct DRG Neurite Outgrowth

Instructive biomaterials capable of controlling the behaviour of the cells are particularly interesting scaffolds for tissue engineering and regenerative medicine. Novel biomaterials are particularly important in societies with rapidly aging populations, where demand for organ/tissue donations is greater than their supply. Herein we describe the preparation of electrically conductive silk film-based nerve tissue scaffolds that are manufactured using all aqueous processing. Aqueous solutions of *Bombyx mori* silk were cast on flexible polydimethylsiloxane substrates with micrometer-scale grooves on their surfaces, allowed to dry, and annealed to impart β -sheets to the silk which assures that the materials are stable for further processing in water. The silk films were rendered conductive by generating an interpenetrating network of polypyrrole and polystyrenesulfonate in the silk matrix. Films were incubated in an aqueous solution of pyrrole (monomer), polystyrenesulfonate (dopant) and iron chloride (initiator), after which they were thoroughly washed to remove low molecular weight components (monomers, initiators, and oligomers) and dried, yielding conductive films with sheet resistances of $124 \pm 23 \text{ k}\Omega \text{ square}^{-1}$. The micrometer-scale grooves that are present on the surface of the films are analogous to the natural topography in the extracellular matrix of various tissues (bone, muscle, nerve, skin) to which cells respond. Dorsal Root Gangions (DRGs) adhere to the films and the grooves in the surface of the films instruct the aligned growth of processes extending from the DRGs. Such materials potentially enable the electrical stimulation of cells cultured on them, and future in vitro studies will focus on understanding the interplay between electrical and topographical cues on the behaviour of cells cultured on them.

Keywords: silk; biomaterials; neural; tissue engineering; topography

1. Introduction

The processability, biocompatibility and biodegradability of natural and recombinant silk proteins make them popular components of biomaterials for drug delivery and tissue engineering. Examples of biomaterials based on silk proteins produced by

silkworms (typically *Bombyx mori* silkworm fibroin (BMF) [1-9], although others have been used)[10], bees [11], caddisfly larvae [12], lacewings [13] and spiders [15-18] have been reported, as indeed have composite materials produced thereof [19]. Silk-based tissue scaffolds in an assortment of materials morphologies (including films, fibers, foams and hydrogels) have demonstrated promise in various niches of tissue engineering (e.g., bone, muscle, nerve and skin) in vitro, and in preclinical trials [1-19].

Instructive biomaterials capable of controlling the behaviour of the cells are particularly interesting for tissue engineering [20-23]. Topographical cues in natural bodily tissues instruct cells to align, as observed in bone, muscle, nerve and other tissues [24,25]. Engineers have drawn inspiration from these observations when developing novel methods to impart biomimetic topographical guidance cues to 2D and 3D biomaterials [24,25].

Kaplan and Omenetto developed a simple soft lithography-based casting technique that enables the fabrication of features smaller than 30 nm in silk fibroin films cast from aqueous solution [26]. Silk films having such intricate 2D or 3D nanoscale or microscale patterns have prospects for use in the biomedical [4,27] and optics industries [26-28]. With a view to their application as novel biomaterials, Kaplan and coworkers have applied such patterned films as instructive biomaterials for bone and nerve tissue regeneration, wherein the hierarchically organized microarchitecture of its cells and extracellular matrix (ECM) are known to be important for the function of the tissue [23].

The ECM of cortical bone and the fibrous rings of cardiac muscle tissue (the annulus fibrosus cordis) is organized as stacks of layers of parallel collagen and mineralized ECM that are rotated approximately 30° relative to the underlying layer. Mesenchymal stem cells (MSCs) cultured on silk films with micrometer-scale grooves

were observed to align with the grooves, the films could be stacked with a 30° rotation relative to the underlying layer, and when cultured in osteogenic medium they differentiated towards osteogenic outcomes [29, 30].

Nervous tissues, such as ocular tissues also contain oriented cells in the central stroma, outermost and innermost endothelium. Human cornea fibroblasts cultured on silk films with micrometer-scale grooves were observed to align with the grooves [31], and modification of such films to display the RGD peptide enhanced cell attachment, proliferation, alignment and the expression of collagen-1, collagen-V, decorin and biglycan [32, 33]. Stacks of such films facilitated the generation of integrated corneal stroma tissue with helicoidal multi-lamellar alignment of collagen-rich and proteoglycan-rich ECM [32]. Moreover, human corneal stromal stem cells cultured on such RGD modified films in serum-free keratocyte differentiation medium successfully differentiated into keratocytes, secreting multilayered lamellae with orthogonally-oriented collagen fibrils, in a pattern mimicking human corneal stromal tissue [34]. Likewise, human corneal limbal epithelial cells were observed to align on silk films with micrometer scale grooves, while also enhancing cell-to-cell contact formation, actin cytoskeleton alignment and focal adhesion localization [35]; and analogous patterns were found to direct the migration of limbal-epithelial cells cultured as sheets [36].

Other nervous tissues such as the brain also contain regions with aligned cells, and patterned silk films with surface micro-grooves of 3 μm in width and 0.5 μm depth have dimensions that are analogous to the dimensions of cortical axons (0.3–1 μm) and glial cell processes (2–3 μm) [37]. Primary E18 rat cortical cells were cultured on silk films with grooves of 3.5 μm in width and 500 nm in depth separated by a 3.5 μm gap were found to align with the grooves. By division 3–5 neuronal (neurofilament, NF⁺)

processes were aligned with the grooves as were glial fibrillary acidic protein (GFAP)+ astrocytes. However, neither axons stained with β 3-tubulin or dendrites stained with microtubule associated protein 2 showed directional preferences [37]. Interestingly, it has also proven possible to integrate gold electrodes into silk films upon which embryonic carcinoma P19 cells (derived from an embryo-derived teratocarcinoma in mice) that were induced to differentiate towards neural-like cells align and increase neurite outgrowth, and such electrode-integrated films offer a potential platform to study electrical stimulation of cells residing on them [38]. Likewise, neurites from dorsal root ganglions (DRGs) and Schwann cell processes grew on films with μ m-scale grooves and showed a majority of extensions within 20° of the groove direction [39]. Furthermore, when human corneal stromal stem cells were co-cultured with DRGs, neurites outgrowth was enhanced by the secretion of collagen-1 from the human corneal stromal stem cells [40].

Conducting biomaterials based on conducting polymers (e.g. polypyrrole) have potential for numerous short and long term biomedical applications [41-49]. Conducting polymer-based scaffolds have been developed for the regeneration of bone and nerve tissues, and organs including the heart and skin [41-49]. Schmidt and Langer showed that electrical stimulation of PC12 cells on polypyrrole increased the number and length of neurite outgrowths from the cells [50]. Various groups have shown that Schwann cells adhere to polypyrrole-based materials [51-55], and that DRGs adhere to polypyrrole-based [51,56,57] or poly(3,4-ethylenedioxythiophene)-based materials [56]. Wang and coworkers showed that flexible tube-like peripheral nerve conduits composed of polypyrrole and silicone were non-toxic and non-immunogenic in vivo in rats [51] and Zhang and coworkers showed that axons could grow into tube-like peripheral nerve conduits composed of poly(D,L-lactide-co- ϵ -caprolactone) [51]. Wallace and coworkers

reported that electrical stimulation enhanced neurite outgrowth from DRGs aligned with the long axis of fibers aligned with the long axis of tubes, and that Schwann cell migration was similarly enhanced [58]; Xia and coworkers showed that electrical stimulation enhanced neurite outgrowth from DRGs aligned with the long axis of aligned bundles of electrospun polypyrrole-based fibers [59], as indeed did Schmidt and coworkers in polypyrrole-based tubes [60]. Schmidt and coworkers showed it was possible to use electrical stimulation to direct Schwann cell migration on polypyrrole-based films [61], and Huang and coworkers reported that electrical stimulation of Schwann cells on composites of polypyrrole and chitosan enhanced the expression and secretion of brain-derived neurotrophic factor and nerve growth factor (NGF) [62], and we have observed enhanced expression of NGF from Schwann cells when stimulated on composites of polypyrrole and polycaprolactone with urea-templated pores [55].

Conductive silk-based materials have been successfully used for biomedical applications, including as electrodes for recording endogenous signals [63], or indeed as tissue scaffolds [64-69]. Here we describe the preparation of films composed of BMF and conducting polymers (polypyrrole doped with polystyrene sulfonate). The films are optionally patterned with micrometer-scale grooves which can direct the growth of neurites in the direction of the long-axis of the groove, analogous to the role of natural topographical cues found in the extracellular matrix of the central and peripheral nervous systems, and such materials may find application in the regeneration of the nervous system acting as scaffolds that guide process outgrowth via topographical cues and facilitate electrical stimulation of the cells on the substrate [70-72].

2. Materials and Methods

2.1. Materials

Unless otherwise stated, all chemicals for synthesis and physicochemical analysis were of ACS grade, purchased from Sigma-Aldrich and used as received without further purification. Phosphate buffered saline (PBS) was at pH 7.4. Reagents for cell culture were purchased from Invitrogen (Carlsbad, CA) unless otherwise noted.

2.2. Preparation of regenerated silk fibroin solution

Silk cocoons of *B. mori* silkworms were degummed by boiling in an aqueous solution of Na₂CO₃ (0.02 M) for 20 min, followed by rinsing thoroughly with distilled water. The extracted silk fibroin was then dissolved in aqueous LiBr (9.3 M), and thereafter dialyzed against ultrapure water using a Slide-a-Lyzer dialysis cassette (MWCO 3,500 Daltons, Life Technologies, Carlsbad, CA, USA) for 2 days. The solution was centrifuged at 9000 rpm (ca. 12,700 g) at 4 °C for 20 min, transferred to a fresh centrifuge tube, and centrifuged at 9000 rpm (ca. 12,700 g) at 4 °C for a further 20 min to remove any solids. The final concentration of silk fibroin aqueous solution was 8 wt%, as determined by dry weight analysis.

2.3. Preparation of PDMS substrates

Flat and patterned silk fibroin films were cast using a previously described soft lithography technique [30]. Flat PDMS substrates were prepared by casting on a Petri dish, whereas grooved PDMS substrates were prepared by casting Sylgard 184 (Dow Corning Corp., Midland, MI, USA) on optical diffraction gratings (Edmund Optics, Inc., Great Barrington, NJ, USA). The PDMS was cured overnight at 60 °C, the substrates were cut into 40 x 40 mm squares, washed in aqueous ethanol (70% v/v

ethanol) and thoroughly rinsed in distilled water, and air dried to yield PDMS films that were either flat or patterned with grooves of 3.5 μm in width and 500 nm in depth separated by a 3.5 μm gap.

2.4. Preparation of silk films

Silk films were prepared by casting 1.2 mL of 1 % w/v regenerated silk fibroin solution on each PDMS substrate and air-dried at room temperature overnight. The resulting 3 to 5 μm thick silk films (either flat or with grooves of 3.5 μm in width and 500 nm in depth separated by a 3.5 μm gap) were made water insoluble by annealing in a water-filled desiccator at 24 mm Hg vacuum for 5 h, followed by drying.

2.5. Preparation of conductive silk films with interpenetrating networks of polypyrrole and polystyrene sulfonate

Pyrrole was purified by passage over basic alumina. Silk films were placed in disposable 50 mL centrifuge tubes containing a solution of pyrrole (291 μL , 4.3 mmol) and polystyrene sulfonate (PSS, Mn 70 kDa, 0.799 g, 1 molar eq. in terms of sulfonate groups to pyrrole) in distilled water (50 mL). Samples were sonicated for 5 minutes and incubated at 4 $^{\circ}\text{C}$ for 1 h. Thereafter, ferric chloride (1.848 g, 2.7 molar eq. relative to pyrrole) was added. The samples were shaken to assure dissolution of the ferric chloride and then incubated for a further 24 h at 4 $^{\circ}\text{C}$. The reaction mixture was decanted and the foams were washed with water, however, the interpenetrating network was inhomogeneous after this time. Therefore, the process was repeated, and a fresh solution of pyrrole (291 μL , 4.3 mmol) and polystyrene sulfonate (PSS, Mn 70 kDa, 0.799 g, 1 molar eq. in terms of sulfonate groups to pyrrole) in distilled water (50 mL) was added to the foams. Samples were sonicated for 5 minutes and cooled to 4 $^{\circ}\text{C}$ (for 1 h). Thereafter, ferric chloride (1.848 g, 2.7 molar eq. relative to pyrrole) was added.

Homogeneously colored films were removed from the reaction mixture, placed in fresh distilled water, sonicated for 5 min, and then exhaustively washed (to remove monomers, oligomers and initiators) with deionized water until the water used to wash the materials was clear, colourless and the pH was neutral (ca. 3 days), after which they were washed with ethanol (1 day at 21°C with two changes of ethanol). Conductive silk films with an interpenetrating network of polypyrrole and polystyrene sulfonate were dried under high vacuum at 21°C.

2.6. Electrical sheet resistance

Resistance (R in Ω) was measured between the two silver electrodes using a digital multimeter (DM-8A, Sperry Instrument, Milwaukee, WI). Sheet resistance (R_s) in Ω/square was calculated using the following equation:

$$R_s = RW/L \quad (1)$$

Where W is the width of the electrode and L is the distance between the two silver electrodes. The electrodes were moved to different positions after each measurement, and the resistance R was recorded in at least ten different positions on the materials.

2.7. Scanning electron microscopy (SEM)

Samples were mounted on a Scanning Electron Microscopy (SEM) stub and sputter coated with Pt/Pd (15 nm) using a Cressington 208 Benchtop Sputter Coater. All samples were imaged using a Zeiss Supra 40 VP field emission scanning electron microscope.

2.8. X-ray photoelectron spectroscopy (XPS)

XPS was carried out on the samples to confirm that the surface chemistry of the

scaffolds had changed after the growth of an interpenetrating network of the CP within the silk matrix. XPS was performed on a Kratos Axis X-ray photoelectron spectrometer (Kratos Analytical Ltd., Manchester, UK). The binding energy was calibrated using the C 1s photoelectron peak at 284.6 eV as a reference. The CasaXPS computer program was used for peak fitting of the C 1s and O 1s peaks in the XPS spectra. The reported spectra are representative of two measurements at different positions on a sample.

2.9. Fourier transform infrared spectroscopy (FTIR)

A Thermo Scientific Nicolet 380 FTIR Spectrometer (Thermo Fisher Scientific Inc., USA) was used to record spectra in attenuated total reflectance (ATR) mode at 21 °C with a 1 cm⁻¹ resolution and 128 scans (corrected for background and atmosphere using the software provided with the spectrometer). Samples were secured in position on the ATR crystal using the built-in clamp.

2.10. Thermogravimetric analysis (TGA)

TGA was conducted on a TA Instruments TGA Q500 thermogravimetric analyzer (TA Instruments, USA), using a ramp rate of (10 °C min⁻¹) under nitrogen gas. Weight loss from the polymers occurring below 200 °C was ascribed to the evaporation of solvents, and above 200 °C it was ascribed to the decomposition of the polymers.

2.11. Cell culture

All primary cell isolation procedures were performed with the approval of the IACUC at the University of Florida and in accordance with guidelines established by the NIH. Whole DRGs were obtained from P1-P3 mice. Briefly, using aseptic techniques, the spinal column was first removed. Next, using a stereomicroscope whole DRGs were pulled out from between each of the spinal segments (from cervical to lumbar). Whole

DRGs were stored and trimmed in 1x HBSS supplemented with 1% gentamicine on ice until ready for use. Isolated and trimmed DRGs were carefully picked up using micro-tweezer (Dumont #5) and dragged through a drop of collagen I solution (3mg/mL, BD Sciences, San Jose, CA). DRG were then placed on the substrates and cultured in neurobasal medium supplemented with 2% B27, 20 nm L-glutamine, 1% penicillin/streptomycin/antimicotic, and 50 ng/ml of nerve growth factor (NGF; R&D Systems, Minneapolis, MN) at 37°C for 3 days in vitro.

2.12. Immunohistochemistry, imaging and analysis

Samples were fixed with 2% paraformaldehyde (PFA) for 30 minutes at room temperature, washed with phosphate buffered saline (PBS), and stored in PBS solution at 4°C. Evaluation of axon growth was performed by immunohistochemistry utilizing antibodies against anti-beta III tubulin (1:1000, Abcam, Cambridge, MA). Goat anti-mouse Alexa Fluor (1:500, Invitrogen) was used as fluorescent secondary antibodies to visualize the location of the primary antibodies. Samples were counter stained with DAPI (1:1000, Invitrogen), a DNA marker to locate cell nuclei. Sections were then cover slipped using a Fluoromount-G (SouthernBiotech, Birmingham, AL) mounting media. The morphology of neurite outgrowth on different substrates was taken on Zen software on a Zeiss (Axio Imager.Z2) machine with an AxioCam HRm Zeiss camera at a magnification of 10x. Quantitative analysis was performed to determine the influence of substrates on neurite direction using Image J (Wayne Rasband, NIMH). Maximum and average lengths of neurites outgrowth were investigated and by fitting an ellipse around the area eccentricity of neurite field was calculated using the following equation:

$$Ecc = \sqrt{(a^2-b^2)}/a \quad (2)$$

In which a and b are major and minor semiaxes respectively. At least three

images of each group were used for quantitative analysis. Angle distribution was also performed in a grooved sample to determine the alignment of the neurite outgrowth by counting 50 fibers on each type of substrate.

2.13. Statistical analysis

A student's two-tailed t-test was used with a statistically significant value determined to be $p < 0.05$.

3. Results and Discussion

3.1. Preparation and characterization of the films

Instructive tissue scaffolds capable of controlling cell behaviour are exciting features in engineering biologically relevant biomaterials [20-22]. The topography of the extracellular matrix of natural bodily tissues can instruct cells to align, and is commonly observed within specific niches in bone, muscle, nerve and other tissues, and this knowledge has been drawn on as a source of inspiration when engineering topographically instructive biomaterials such as those described herein [24,25]. Natural and recombinant silk proteins are popular components of biomaterials because of their solubility in various solvents and ease of processing into films, fibers, foams, hydrogels etc. [1, 5, 14, 18, 19]. The Kaplan group and others have developed silk-based materials for soft and hard tissues, and such materials show excellent biocompatibility both in vitro and in preclinical trials in animals [1-3]. Many tissues respond to electrical stimulation (including bone, muscle, nerve, skin), and a variety of devices employing electrical stimulation for therapeutic purposes have been translated to the clinic [44-47]. Here we describe the preparation and physicochemical characterization of conductive silk films, optionally with topographical instructions in their surfaces [30].

Optically clear flat and patterned silk fibroin films were prepared by casting on flat or patterned PDMS substrates [30]. Incubation of the silk films in an aqueous solution of pyrrole (monomer), polystyrenesulfonate (dopant) and ferric chloride (initiator), followed by thorough washing with water and ethanol to remove the by-products (e.g. initiators, monomers, oligomers and polymers) and vacuum drying, yielded conductive silk films with sheet resistances of $124 \pm 23 \text{ k}\Omega \text{ square}^{-1}$. Thermogravimetric analysis revealed that the chemical modification process did not alter the thermal stability of the films significantly (Appendix, Figure A1). SEM showed that the surface of the non-conductive silk films are smooth (Figure 1A and 1C), and that the conductive films are coated with aggregates of polypyrrole and polystyrenesulfonate on their surface and are therefore notably rougher (Figure 1B and 1D) [55].

Infrared spectra recorded in ATR mode of the non-conductive silk films and the conductive silk films (Figure 2A) confirmed the surface chemistry to be different. The infrared spectrum for both the non-conductive and conductive silk films exhibit peaks at 1621 cm^{-1} and 1517 cm^{-1} corresponding to the amide I and amide II peaks, respectively, indicating the silk film is β -sheet rich. The peak at 925 cm^{-1} is attributed to pyrrole C-H wagging, the peak at 1033 cm^{-1} is attributed to C-H in-plane deformation and/or symmetric S=O stretching, the peak at 1203 cm^{-1} is attributed to asymmetric S=O stretching, the shoulders at 1487 cm^{-1} and 1558 cm^{-1} correspond to the C=C stretching, whereas the shoulder at 1688 cm^{-1} is C=N bonds [73]. X-ray photoelectron spectra of the non-conductive and conductive films also confirms that the surface chemistry is different, with the broadening of the N1s peak in the spectra of the conductive films at 400 eV because of the newly introduced nitrogen on the pyrrole rings (Figure 2B) and the appearance of a new peak in the S2p spectra of the conductive films at 168 eV from

the polystyrenesulfonate (Figure 2C) [55]. In conclusion, microscopy and spectroscopy showed clear evidence of the deposition of aggregates of polyelectrolyte complexes formed from polypyrrole and polystyrene sulfonate on the silk films, confirming that the conductivity of the materials is due to the presence of the conducting polymer.

3.2. In vitro culture of DRGs on conducting substrates

While such materials have the potential for use in any of the biological niches mentioned above, as proof of concept, we focused on nerve tissues. In this study, DRGs were cultured on the surface of the conductive films for 3 days in vitro. Two conditions were considered: 1) DRGs seeded on flat conductive silk films, and 2) DRGs seeded on conductive silk films with grooves. Histological analysis of processes produced from the DRGs after 3 days in vitro showed that the conductive films with grooves substrates instructed the alignment of the processes extending from the DRGs, producing significantly more aligned processes when compared to processes extending from DRGs cultured on flat conductive silk substrates ($p < 0.04$). While there was a trend towards longer neurites on grooved substrates, no significant differences were seen in the average or maximum lengths in process outgrowth (Figure 3 and Appendix Figure A2).

Nerve tissue engineering is an exciting field of research, and silk proteins are a class of materials that has shown great promise both in vitro and in vivo in preclinical trials [3]. Herein we report the first study of a conducting silk derivative and its application as a topographically instructive nerve tissue scaffold which may find use in fundamental studies investigating effects of topographical and electrical cues at the same time, with a long term view to optimize combinations of cues (chemical, electrical, mechanical, and topographical) and generate advanced functional

biointerfaces for the central and peripheral nervous systems.

4. Conclusion

In summary, we present a protocol to prepare conductive silk films (optionally with topographical guidance cues) using simple, scalable, all-aqueous methods. DRGs adhere to the films and the topographical information in the surface of the conductive silk films (μm -scale grooves) instructs the aligned growth of processes extending from the DRGs. Such materials potentially enable the electrical stimulation of cells cultured on them, and future in vitro studies will focus on understanding the interplay between electrical and topographical cues on the behaviour of cells cultured on them [74,75].

Acknowledgements

We thank the University of Texas at Austin for financial support in the form of a Special Research Grant to facilitate the initiation of this collaborative research project, and support of D. J. M. and R. C. S. in the form of Undergraduate Research Fellowships. At the Department of Chemistry at the University of Texas at Austin we thank Prof. C. Grant Willson for access to TGA apparatus and Prof. Michael J. Krische for access to an IR spectrometer. SEM was carried out at the Institute for Cellular and Molecular Biology core lab located at the University of Texas at Austin. We thank the University of Florida for financial support in the form of startup resources to C. E. S.

References:

1. Altman, G. H.; Diaz, F.; Jakuba, C.; Calabro, T.; Horan, R. L.; Chen, J.; Lu, H.; Richmond, J.; Kaplan, D. L. *Biomaterials* **24**, 401 (2003).
2. Wang, Y.; Kim, H. J.; Vunjak-Novakovic, G.; Kaplan, D. L. *Biomaterials* **27**, 6064 (2006).
3. Kundu, B.; Rajkhowa, R.; Kundu, S. C.; Wang, X. *Adv. Drug Delivery Rev.* **65**, 457 (2013).

- 4 Borkner, C. B.; Elsner, M. B.; Scheibel, T. *ACS Appl. Mater. Interfaces* **6**, 15611 (2014).
- 5 Hardy, J. G.; Römer, L. M.; Scheibel TR. *Polymer* **49**, 4309 (2008).
- 6 Hardy, J. G.; Scheibel, T. R. *Biochem. Soc. Trans.* **37**, 677 (2009).
- 7 Preda, R. C.; Leisk, G., Omenetto, F., Kaplan, D. L. *Methods Mol. Biol.* **996**, 19 (2013).
- 8 Cao, Y.; Wang, B. *Int. J. Mol. Sci.* **10**, 1514 (2009).
- 9 Zhao, Z.; Li, Y.; Xie, M. B. *Int. J. Mol. Sci.* **16**, 4880 (2015).
- 10 Kundu, S. C.; Kundu, B.; Talukdar, S.; Bano, S.; Nayak, S.; Kundu, J.; Mandal, B. B.; Bhardwaj, N.; Botlagunta, M.; Dash, B. C.; Acharya, C.; Ghosh, A.K. Invited review nonmulberry silk biopolymers. *Biopolymers* **97**, 455 (2012).
- 11 Sutherland, T. D.; Church, J. S.; Hu, X.; Huson, M. G.; Kaplan, D. L.; Weisman, S. *PLoS One* **6**, e16489 (2011).
- 12 Addison, J. B.; Ashton, N. N.; Weber, W. S.; Stewart, R. J.; Holland, G. P.; Yarger, J. L. *Biomacromolecules* **14**, 1140 (2013).
- 13 Bauer, F.; Scheibel, T. *Angew. Chem. Int. Ed. Engl.* **51**, 6521 (2014).
- 14 Widhe, M.; Johansson, J.; Hedhammar, M.; Rising, A. *Biopolymers* **97**, 468 (2012).
- 15 Radtke, C.; Allmeling, C.; Waldmann, K. H.; Reimers, K.; Thies, K.; Schenk, H. C.; Hillmer, A.; Guggenheim, M.; Brandes, G.; Vogt, P. M. *PLoS One* **6**, e16990 (2011).
- 16 Schacht, K.; Scheibel, T. *Curr. Opin. Biotechnol.* **29**, 62 (2014).
- 17 Hardy, J. G.; Scheibel, T. R. *J. Polym. Sci. A: Polym. Chem.* **47**, 3957 (2009).
- 18 Rising, A.; Widhe, M.; Johansson, J.; Hedhammar, M. *Cell. Mol. Life Sci.* **68**, 169 (2011).
- 19 Hardy, J. G.; Scheibel, T. R. *Prog. Polym. Sci.* **35**, 1093 (2010).

- 20 Lutolf, M. P.; Hubbell, J. A. *Nat. Biotechnol.* **23**, 47 (2005).
- 21 Place, E. S.; Evans, N. D.; Stevens, M. M. *Nat. Mater.* **8**, 457 (2009).
- 22 Abbott, R. D.; Kaplan, D. L. *Trends Biotechnol.* **33**, 401 (2015).
- 23 Torres-Rendon, J. G.; Femmer, T.; De Laporte, L.; Tigges, T.; Rahimi, K.; Gremse, F.; Zafarnia, S.; Lederle, W.; Ifuku, S.; Wessling, M.; Hardy, J. G.; Walther, A. *Adv. Mater.*, **27**, 2989 (2015).
- 24 Curtis, A. S.; Wilkinson, C. D. *J. Biomater. Sci. Polym. Ed.* **9**, 1313 (1998).
- 25 Li, Y.; Huang, G.; Zhang, X.; Wang, L.; Du, Y.; Lu, T. J.; Xu, F. *Biotechnol. Adv.* **32**, 347 (2014).
- 26 Perry, H.; Gopinath, A.; Kaplan, D. L.; Dal Negro, L.; Omenetto, F. G. *Adv. Mater.* **20**, 3070 (2008).
- 27 Omenetto, F. G.; Kaplan, D. L. *Nature Photon.* **2**, 641 (2008).
- 28 Pal, R. K.; Kurland, N. E.; Wang, C.; Kundu, S. C.; Yadavalli, V. K. *ACS Appl. Mater. Interfaces* **7**, 8809 (2015).
- 29 Sengupta, S.; Park, S. H.; Seok, G. E.; Patel, A.; Numata, K.; Lu, C. L.; Kaplan, D. L. *Biomacromolecules* **11**, 3592 (2010).
- 30 Tien, L. W.; Gil, E. S.; Park, S. H.; Mandal, B. B.; Kaplan, D. L. *Macromol. Biosci.* **12**, 1671 (2012).
- 31 Gil, E. S.; Park, S. H.; Marchant, J.; Omenetto, F.; Kaplan, D. L. *Macromol. Biosci.* **10**, 664 (2010).
- 32 Gil, E. S.; Mandal, B. B.; Park, S. H.; Marchant, J. K.; Omenetto, F. G.; Kaplan, D. L. *Biomaterials* **31**, 8953 (2010).
- 33 Jia, L.; Ghezzi, C. E.; Kaplan, D. L. *J. Biomed. Mater. Res. Part B Appl. Biomater.* DOI: 10.1002/jbm.b.33408 (2015).

- 34 Wu, J.; Rnjak-Kovacina, J.; Du, Y.; Funderburgh, M. L.; Kaplan, D. L.; Funderburgh, J. L. *Biomaterials* **35**, 3744 (2014).
- 35 Lawrence, B. D.; Pan, Z.; Liu, A.; Kaplan, D. L.; Rosenblatt, M. I. *Acta Biomater.* **8**, 3732 (2012).
- 36 Lawrence, B. D.; Pan, Z.; Rosenblatt, M. I. *PLoS One* **7**, e50190 (2012).
- 37 Tang-Schomer, M. D.; Hu, X.; Tupaj, M.; Tien, L. W.; Whalen, M.; Omenetto, F.; Kaplan, D. L. *Adv. Funct. Mater.* **24**, 1938 (2014).
- 38 Hronik-Tupaj, M.; Raja, W. K.; Tang-Schomer, M.; Omenetto, F. G.; Kaplan, D. L. *J. Biomed. Mater. Res. A* **101**, 2559 (2013).
- 39 White, J. D.; Wang, S.; Weiss, A. S.; Kaplan, D. L. *Acta Biomater.* **14**, 1 (2015).
- 40 Wang, S.; Ghezzi, C. E.; White, J. D.; Kaplan, D. L. *J. Biomed. Mater. Res. A*. doi: 10.1002/jbm.a.35465 (2015).
- 41 Guo, B.; Glavas, L.; Albertsson, A. C. *Prog. Polym. Sci.* **38**, 1263 (2013).
- 42 Bendrea, A. D.; Cianga, L.; Cianga, I. *J. Biomater. Appl.* **26**, 3 (2011).
- 43 Ghasemi-Mobarakeh, L.; Prabhakaran, M. P.; Morshed, M.; Nasr-Esfahani, M. H.; Baharvand, H.; Kiani, S.; Al-Deyab, S. S.; Ramakrishna, S. *J. Tissue Eng. Regen. Med.* **5**, e17 (2011).
- 44 Green, R. A.; Lovell, N. H.; Wallace, G. G.; Poole-Warren, L. A. *Biomaterials* **29**, 3393 (2008).
- 45 Muskovich, M.; Bettinger, C. J. *Adv. Healthc. Mater.* **1**, 248 (2012).
- 46 Hardy, J. G.; Lee, J. Y.; Schmidt, C. E. *Curr. Opin. Biotechnol.* **5**, 847 (2013).
- 47 Thompson, D. M.; Koppes, A. N.; Hardy, J. G.; Schmidt, C. E. *Annu. Rev. Biomed. Eng.* **16**, 397 (2014).

- 48 Pillay, V.; Tsai, T. S.; Choonara, Y. E.; du Toit, L. C.; Kumar, P.; Modi, G., Naidoo, D.; Tomar, L. K.; Tyagi, C.; Ndesendo, V. M. *J. Biomed. Mater. Res. A* **102**, 2039 (2014).
- 49 Hardy, J. G.; Mouser, D. J.; Arroyo-Currás, N.; Geissler, S.; Chow, J. K.; Nguy, L.; Kim, J. M.; Schmidt, C. E. *J. Mater. Chem. B* **2**, 6809 (2014).
- 50 Schmidt, C. E.; Shastri, V. R.; Vacanti, J. P.; Langer, R. *Proc. Natl. Acad. Sci. USA* **94** 8948 (1997).
- 51 Wang, X.; Gu, X.; Yuan, C.; Chen, S.; Zhang, P.; Zhang, T.; Yao, J.; Chen, F.; Chen, G. *J. Biomed. Mater. Res. A* **68**, 411 (2004).
- 52 Fonner, J. M.; Forciniti, L.; Nguyen, H.; Byrne, J. D.; Kou, Y. F.; Syeda-Nawaz, J.; Schmidt, C. E. *Biomed. Mater.* **3**, 034124 (2008).
- 53 Lee, J. Y. *Polym. Rev.* **24**, 847 (2013).
- 54 Lee, J. Y.; Schmidt, C. E. *J. Biomed. Mater. Res. A* **103**, 2126 (2015).
- 55 Hardy, J. G.; Cornelison, R. C.; Sukhavasi, R. C.; Saballos, R. J.; Vu, P; Kaplan, D. L.; Schmidt, C. E. *Bioengineering* **2**, 15 (2015).
- 56 Abidian, M. R.; Corey, J. M.; Kipke, D. R.; Martin, D. C. *Small* **6**, 421 (2010).
- 57 Runge, M. B.; Dadsetan, M.; Baltrusaitis, J.; Knight, A. M.; Ruesink, T.; Lazcano, E. A.; Lu, L.; Windebank, A. J.; Yaszemski, M. J. *Biomaterials* **31**, 5916 (2010).
- 58 Quigley, A. F.; Razal, J. M.; Thompson, B. C.; Moulton, S. E.; Kita, M.; Kennedy, E. L.; Clark, G. M.; Wallace, G. G.; Kapsa, R. M. *Adv. Mater.* **21**, 4393 (2009).
- 59 Xie, J.; Macewan, M. R.; Willerth, S. M.; Li, X.; Moran, D. W.; Sakiyama-Elbert, S. E.; Xia, Y. *Adv. Funct. Mater.* **19**, 2312 (2009).
- 60 Nguyen, H. T.; Sapp, S.; Wei, C.; Chow, J. K.; Nguyen, A.; Coursen, J.; Luebben, S.; Chang, E.; Ross, R.; Schmidt, C. E. *J. Biomed. Mater. Res. A* **102**, 2554 (2014).

- 61 Forciniti, L.; Ybarra, J. 3rd; Zaman, M. H.; Schmidt, C. E. *Acta Biomater.* **10**, 2423 (2014).
- 62 Huang, J.; Hu, X.; Lu, L.; Ye, Z.; Zhang, Q.; Luo, Z. *J. Biomed. Mater. Res. A.* **93**, 164 (2010).
- 63 Tsukada, S.; Nakashima, H.; Torimitsu, K. *PLoS One.* **7**, e33689 (2012).
- 64 Müller, C.; Jansson, R.; Elfving, A.; Askarieh, G.; Karlsson, R.; Hamed, M.; Rising, A.; Johansson, J.; Inganäs, O.; Hedhammar, M. *J. Mater. Chem.*, **21**, 2909 (2011).
- 65 Cucchi, I.; Boschi, A.; Arosio, C.; Bertini, F.; Freddi, G.; Catellani, M. *Synth. Metals* **159**, 246 (2009).
- 66 Aznar-Cervantes, S.; Roca, M. I.; Martinez, J. G.; Meseguer-Olmo, L.; Cenis, J. L.; Moraleda, J. M.; Otero, T. F. *Bioelectrochemistry* **85**, 36 (2012).
- 67 Xia, Y.; Lu, X.; Zhu, H. *Comp. Sci. Technol.* **77**, 37 (2013).
- 68 Zhang, J.; Qiu, K.; Sun, B.; Fang, J.; Zhang, K.; El-Hamshary, H.; Al-Deyab, S. S.; Mo, X. *J. Mater. Chem. B*, **2**, 7945 (2014).
- 69 Hardy, J. G.; Geissler, S. A.; Aguilar Jr., D.; Villancio-Wolter, M. K.; Mouser, D. J.; Sukhvasi, R. C.; Cornelison, R. C.; Tien, L. W.; Preda, R. C.; Hayden, R. S.; Chow, J. K.; Nguy, L.; Kaplan, D. L.; Schmidt, C. E. *Macromol. Biosci.* DOI: 10.1002/mabi.201500171 (2015).
- 70 Hoffman-Kim, D.; Mitchel, J. A.; Bellamkonda, R. V. *Annu. Rev. Biomed. Eng.* **12**, 203 (2010).
- 71 Spivey, E. C.; Khaing, Z. Z.; Shear, J. B.; Schmidt, C. E. *Biomaterials* **33**, 4264 (2012).
- 72 Khaing, Z. Z.; Schmidt, C. E. *Neurosci. Lett.* **519**, 103 (2012).
- 73 Chougule, M. A.; Pawar, S. G.; Godse, P. R.; Mulik, R. N.; Sen, S.; Patil, V. B. *Soft Nanosci. Lett.* **1**, 6 (2011).

74 Gomez, N.; Chen, S.; Schmidt, C. E. *J. R. Soc. Interface* **4**, 223 (2007).

75 Gomez, N.; Lu, Y.; Chen, S.; Schmidt, C. E. *Biomaterials* **28**, 271 (2007).

Figure 1. SEM images of the films. A) Flat non-conductive silk film. B) Flat conductive silk film. C) Non-conductive silk film with grooves. D) Conductive silk film with grooves. Scale bars represent 10 μm .

Figure 2. A) FTIR spectra of non-conductive and conductive silk films. B) XPS (N1s) spectra of non-conductive and conductive silk films. C) XPS (S2p) spectra of non-conductive and conductive silk films. Gray and black lines correspond to non-conductive and conductive silk films, respectively.

Figure 3. Neurites grew along the aligned features on conductive silk films. Dorsal root ganglia (DRG) were isolated and placed on either grooved (A) or flat silk conductive films and cultured for 3 days in vitro. A & B. Photomicrographs of fixed samples that were stained with neuronal marker (beta III tubulin, red) and imaged. C. An overlaid image of labelled axons with a phase contrast image of the underlying grooved substrate (feature size = 3.5 μm). Scale bar = 500 μm .

Into The Groove: Instructive Conductive Silk Films With Topological Guidance Cues Direct DRG Neurite Outgrowth

Supplementary Information

Figure A1. Thermogravimmetric analysis of silk-based films. Grey) Silk. Black) Silk-PPy.

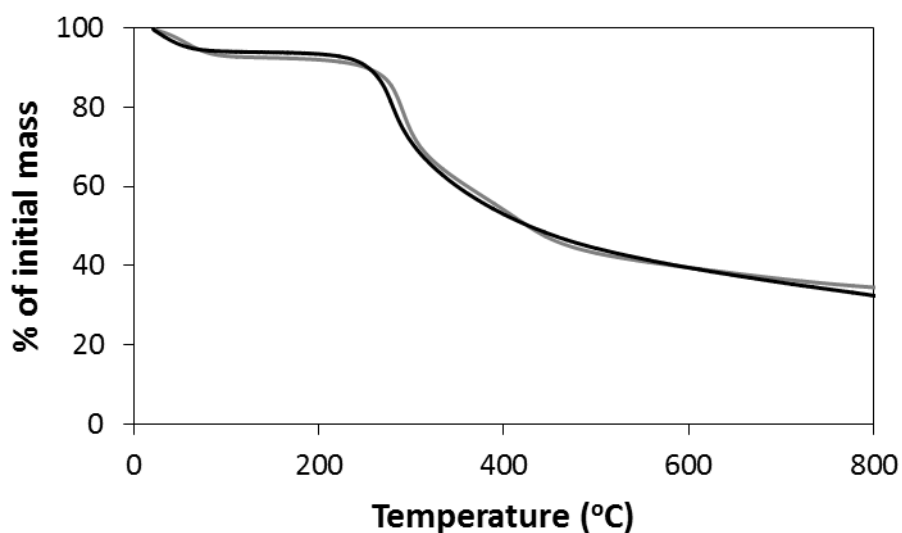


Figure A2. Quantitative analysis of neurites from dorsal root ganglia (DRG) cultured in vitro on conductive silk films. A) Average length and B) maximum length of neurites were calculated from DRGs grown on both flat and grooved substrates (flat: n= 5, grooved: n=4). C) A histogram of angle distribution for neurites on grooved substrates (n > 50 neurites on from 4 DRGs).

